Comprehensive Journal of Science
Volume (11), Issue (42), (Sapt, 2026)
ISSN: 3104-6266

مجلة العلوم الشاملة
المجلد (11) العدد 42 سبتمبر 2026
ردمد: 3104-6266

DEVELOPMENT OF A MATHEMATICAL MODEL TO IMPROVE THE GAS DYNAMIC PROTECTION OF PLASMATRON CATHODE ASSEMBLIES

Alkeeb Ahmed M. Mohammed Aljali[1], Nahla Faiz Abdullah Al Dabagh[2]
[1].Higher Institute of Science and Technology, Suq Aljumuea
,[2]. Higher Institute of Science and Technology, Tripoli
Corresponding Email. 1.ah87ah@yahoo.com , 2.Nahla Faiz5@gmail.com
Received: 08/9/2026 Revised: 13/9/2026 Accepted: 05/10/2026 Publication: 05/11/2026

Abstract
The article analyzes the main approaches to mathematical modeling of physical processes in plasma. It is proposed and develop a mathematical model based on the magnetogasdynamic approach to describe plasma. As a result of the comparative analysis of existing turbulence models and comparing the results of simulations with the works of other authors and the results of experiments, it has been chosen SAS - SST model of turbulence. The comparative analysis of the results of simulation of a free-flaming electric arc of atmospheric pressure has shown an acceptable quantitative and qualitative agreement of the obtained result with the experimental data. Tolerance was up to 6% for temperature values and up to 3% for maximum velocity values at arc axis.

Key words: plasma; plasmatron; gas-dynamic protection; cathode assembly; mathematical simulation of plasma flows; SAS - SST model of turbulence.

Introduction

One of the main tasks of the theoretical study of plasma processes is to determine the local physical parameters of the plasma and to establish their relationship with the external energy and geometrical parameters of the plasmatron. Generally, engineering problems require the formation of a certain distribution of plasma temperatures and flows that meets the specific conditions of practical use. This is usually achieved by varying the current intensity, the plasma gas flow rate, the generator operating mode and the plasmatron geometry. That is only by adjusting the external parameters of the plasmatron.

A significant leap in the use of plasma can be achieved by direct control of plasma flows. This problem can be solved by means of mathematical simulation, where different mathematical models describing physical processes in plasma are used to investigate a real object.

There are three main methods of theoretical description of plasma processes: microscopic description using drift approximation; statistical description based on solution of kinetic equations together with Maxwell equations, and macroscopic description using magnetogasdynamic equations.

For the design problems of gas-dynamic protection of cathode assemblies, the macroscopic description is the most common, which is the most justified from the point of view of cost-effectiveness of calculations. The use of other approaches is difficult. Thus, practical study on the basis of kinetic equations faces significant mathematical and computational difficulties due to the fact that this system is already a set of equations in four-dimensional phase space for two-dimensional problems [1].

The existing methods for calculating the modes of gas-dynamic protection of thermocathodes are based on the equations of gas dynamics. However, in practice such methods do not allow to obtain information about a significant number of parameters determining the operation of plasma equipment. From the point of view of thermocathode protection, the main question is the reasonable

assignment of critical partial pressure value. In the works [1, 2], as such a value it is suggested to use air pressure, at which the emission current decreases to the value of 0.75...0.8 of the emission current in vacuum. This choice is justified by steeply falling character of dependence of the thermal emission current value on the air pressure. However, the critical partial pressure value (P_{cr}) depends on the emitter temperature. Therefore, from the physical point of view, the critical partial pressure for the thermocathode should be considered as the value at which there is a transition from the diffuse form of the arc binding to the contracted one. At this transition, there is a sharp increase in the specific heat flows into the cathode and, as a consequence, a spike in the emitter erosion.

This transition will be influenced not only by the properties of the emitter material, but also by geometry of the cathode assembly, the gases velocity and parameters of the electric field in the cathode sheath. For more accurate simulation and understanding of the essence of physical processes occurring near electrodes, it is necessary to consider the equations of flow of multicomponent medium in magnetogasdynamic (MGD) formulation, taking into account the action of electric and magnetic fields.

Purpose

To develop a mathematical model to describe physical processes in plasma based on the magnetogasdynamic approach.

Research methodology

The studied mathematical model is applicable to dense plasma, where the free path length of particles λ is small compared to the characteristic spatial scale L (Knudsen number $K_n = \lambda/L << 1$), and the characteristic duration of processes T is large compared to the time τ between particle collision. In this case, the distribution functions can be represented as sums of series on small parameters λ/L and τ/T with Maxwell function as the zero expansion term [3]. Then, magnetohydrodynamic equations can be derived as equations for the moments of the distribution functions.

Also the mathematical description is based on the MGD approach to plasma as a continuous medium based on gas-dynamic equations, Maxwell equations and relations for thermodynamic parameters in ionized gas.

The model is obtained taking into account the following assumptions (except for the cathode sheath):

- The plasma is assumed to be quasi-neutral. Three types of interaction between particles are realized in plasma, namely: “charge – charge”, “charge - neutral atom”, “neutral atom - neutral atom”. Interactions of the “charge – charge” type are caused by electrostatic forces. Other interactions are caused by forces of quantum-mechanical nature. Local deviations in the concentration of charged particles lead to electric fields in plasma, which prevent further charge separation. Due to this, the condition of quasi-neutrality is fulfilled in plasma on the macroscopic level: $n_e = n_i$ or $n_e = \Sigma\ (Z_a\ n_a)_a$ in the case of multi-charge ions or multi-component plasma. Here n_e, n_i are concentrations of electrons and ions, respectively.
- The plasma is assumed to be thermally equilibrium – electric arcs are characterized by a low degree of ionization, so that the arc plasma has a high electrical resistance, with the result that joule heat generation plays a prominent role in heat transfer. This process leads to an increase in the gas temperature and contributes to the temperature convergence of its components.

- The gas composition in thermodynamic equilibrium can be determined through the thermodynamic parameters of the gas. Ionization equilibrium in plasma is described on the basis of the Saha equation:

$$n_e\left(\frac{n_r}{n_{r-1}}\right)=2\frac{g_r}{g_{r-1}}\left(\frac{2\pi m_e kT_e}{h^2}\right)^{3/2}\exp\left(-\frac{U_1-\Delta U_1}{kT_e}\right), \quad (1)$$

where g is the statistical sum; m_e is the electron mass; T is the absolute temperature of the gas particles; U is the energy required to remove electrons from a neutral atom.

- In plasma, Ohm's law is valid in its simplest form $j = \sigma \bar{E}$, where j is the emission current density; σ is the electrical conductivity of gas; E is the electric field strength.
- The expression for the pressure can be written as the sum of pressures of individual components

$$p=\sum_a n_a kT_a + n_e kT_e, \quad (2)$$

where k – Boltzmann constant.

- The mechanism of electron emission is assumed to be thermo-emission following Richardson's law:

$$j_e = A\cdot T^2\cdot\exp(-\frac{e\varphi}{kT}). \quad (3)$$

where e is the electron charge; A is the thermoelectric constant; φ is the electron work function (potential) from the cathode.

Taking into account the above assumptions (1) - (3), it is assumed that the plasma is in the state of local thermodynamic equilibrium (LTE) and in each investigated region is characterized by two thermodynamic parameters: temperature and pressure. In the frames of this very approximation, the plasma processes have been studied in this work.

The equations for this model are obtained from the corresponding general moment equations (4) - (6) and are written down as follows:

$$\frac{\partial\rho}{\partial t}+\nabla\cdot(\rho u)=0, \quad (4)$$

$$\frac{\partial(\rho u)}{\partial t}+\nabla\cdot(\rho u\times u)=-\nabla P-\nabla\cdot\tau+j\times B+qE.$$

The electric and magnetic field strengths are found from Maxwell's equations:

$$div\,D=\rho_e,\ div\,B=0,\ rot\,E=-\frac{\partial B}{\partial t},\ rot\,H=j, \quad (5)$$

where D – electric induction; ρ_e – суммарный заряд; B – magnetic induction; H – magnetic field strength.

The energy balance equation is used to determine the temperature:

$$\frac{\partial(\rho H)}{\partial t} - \frac{\partial p}{\partial t} + \nabla \cdot (\rho u H) = \\ = \nabla(\lambda \nabla T) + \nabla \cdot (u \cdot \tau) + u \cdot S_u + \frac{j^2}{} - U_{rad} \,. \tag{6}$$

$$U_{rad} = 1.14e^{-40}\sqrt{T}\exp\left(-\frac{\Delta E_i}{kT}\right) n_e \left[n_i \exp\left(\frac{h\nu}{kT} + 4n_{2i}\exp\left(\frac{h\nu^+}{kT}\right)\right)\right],$$

Where $h\nu$ = 2,85 $e\nu$; $h\nu^+$ = 8,2 $e\nu$; ΔE_i – reduced ionisation potential; R_D – Debye radius; ρ – density; p – pressure; u – gas velocity.

The value U_{rad} included in (6) represents the total radiation of the argon plasma, which was modelled as a negative bulk source. In order to determine dependence of the total radiation on the temperature, it was used the calculation method presented in the work [1].

Expression (6) describes the radiant losses due to braking and recombination radiation, as well as discrete transitions between excited states of atom and ion. The calculation result for an equilibrium argon plasma using this formula is given in Fig. 1.

It is well known that the system of Reynolds-averaged Navier-Stokes equations (4) is closed by turbulence equations. However, the variety of existing approaches to describing flows requires a more detailed consideration of the main of them and a reasonable choice of a turbulence model that will meet the requirements depending on specifics of the object studied. A detailed analysis of applicability of the various approaches for calculating flows is presented below.

Let's consider peculiarities of simulation of flows in gas discharge channels of plasmatrons.

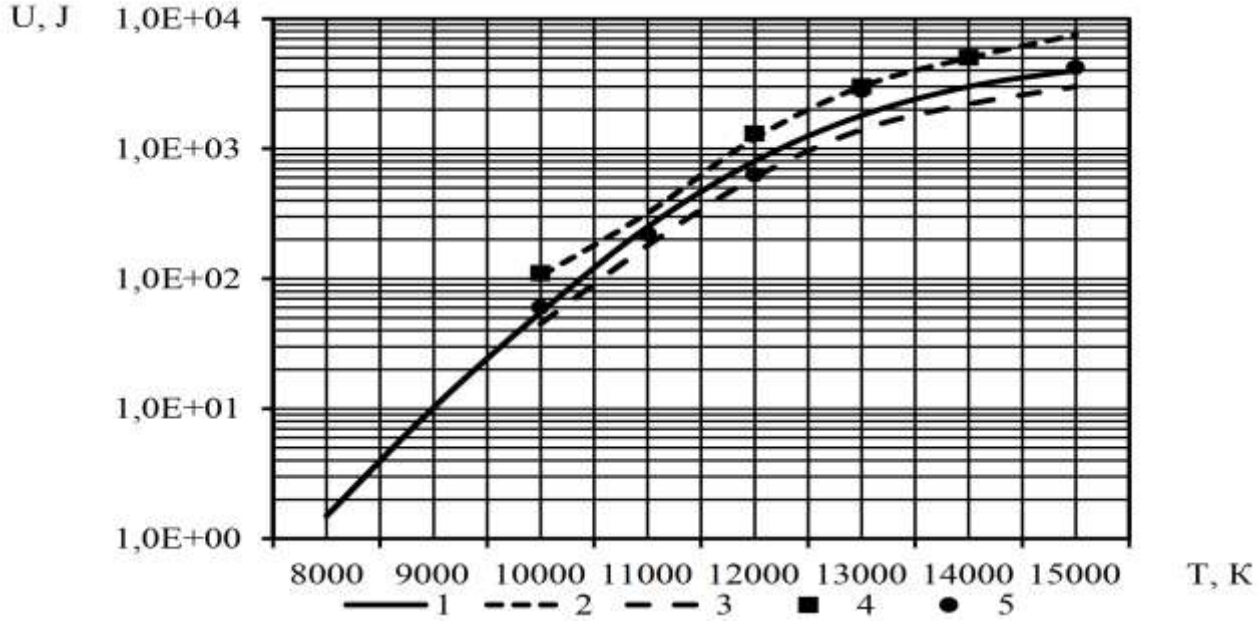


Figure 1 – Total radiation of equilibrium argon plasma depending on temperature at atmospheric pressure:
1, 2, 3, 4 – experimental data; 5, 6, 7 – calculated data

When investigating plasma gas flows in electric arc devices, the following main features of the simulated system take place:

- multicomponent nature;
- complex geometrical flow regions;
- availability of additional equations to describe electrical characteristics of the arc;
- essential non-linearity of the equations, first of all, due to dependence of transfer coefficients on temperature;
- heterogeneity of the flow character.

Consequently, the main criteria for choosing a turbulence model should be: ability to represent correctly the flow pattern with flow detachment and formation of discrete vortex; the turbulence model should not be computationally demanding and the solution should have little dependence on the quality of the finite-element grid.

Numerical calculations have traditionally used turbulence models based on averaged Reynolds equations. The most common are the RNG k-ε, SA and SST turbulence models. They are justified from the point of view of saving computational resources, they are not sensitive to the grid quality, and allow to obtain reliable results for discontinuous flows in most cases.

Let's consider existing models of turbulence in plasma. In the electric arc plasma generators, both laminar and turbulent gas flow modes can be realised. Therefore, a mathematical model of gas flow in the cavity of cathode node should take into account both of these modes. Although the solution of non-stationary Navier-Stokes equations gives an opportunity to describe real turbulent flows, practical investigation of turbulence by methods of direct numerical simulation using the system of Navier-Stokes equations is difficult today because of high computational costs.

As an alternative approach, the Reynolds averaging method (RANS models) is currently the most widely used. It is assumed that the averaged values of the ripple components are zero, but the average of products of fluctuating components are not equal to zero. In averaged motion equations, additional terms (Reynolds stresses) appear, which describe the change of momentum caused by the interaction of turbulent velocity pulsations. To determine the Reynolds stresses, the Boussinesq hypothesis [4] is usually used which relates them to the averaged velocity gradients:

$$-\rho\overline{v_i'v_j'} = \mu_т\left(\frac{\partial v_i}{\partial x_j}+\frac{\partial v_j}{\partial x_i}\right)-\frac{2}{3}\left(\rho k+\mu_т\frac{\partial v_i}{\partial x_i}\right)\delta_{ij}, \qquad (7)$$

$$\mu = \mu_L + \mu_T,\ \lambda = \lambda_L + \lambda_T.$$

The resulting equations describe the behaviour of the averaged characteristics of turbulent flow if the effective values equal to the sum of molecular (laminar dynamic) and turbulent viscosity and thermal conductivity respectively are taken as viscosity μ and thermal λ conductivity coefficients.

To determine μ_T and λ_T, there are numerous semi-empirical theories of turbulence, which can be conditionally subdivided into algebraic and differential models. We limit to analyzing the applicability of those turbulence models, which are implemented in existing commercial CFD packages, to the problems in question. The two-parameter k-ε and k-ω models and their modifications are currently the most widely used among them.

In the classical k-ε Lander-Jones model [5], the turbulent viscosity in the system of equations (7) is determined from the Kolmogorov relation:

$$\mu_т = \frac{C_\mu f_\mu \rho k^2}{\varepsilon}, \tag{8}$$

where k – kinetic energy of turbulent fluctuations; ε – turbulent energy dissipation rate; $C_\mu = 0{,}09$ – model empirical constant; f_μ – function of turbulent Reynolds number.

In order to determine the kinetic energy of turbulence and its dissipation rate, two additional equations are used in the k-ε model:

$$\frac{\partial \rho k}{\partial t} + \frac{\partial}{\partial x_i}(\rho v_i k) = \frac{\partial}{\partial x_i}\left(\left(\mu_л + \frac{\mu_т}{\sigma_k}\right)\frac{\partial k}{\partial x_i}\right) + S_k, \tag{9}$$

$$\frac{\partial \rho \varepsilon}{\partial t} + \frac{\partial}{\partial x_i}(\rho v_i \varepsilon) = \frac{\partial}{\partial x_i}\left(\left(\mu_л + \frac{\mu_т}{\sigma_\varepsilon}\right)\frac{\partial \varepsilon}{\partial x_i}\right) + S_\varepsilon,$$

where

$$S_k = \tau_{ij}\frac{\partial v_i}{\partial x_j} - \rho\varepsilon + \mu_л P_в;$$

$$S_\varepsilon = C_{\varepsilon 1}\frac{\varepsilon}{k}\left(f_1 \tau_{ij}\frac{\partial v_i}{\partial x_j} + \mu_т C_в P_в\right) - C_{\varepsilon 2} f_2 \frac{\rho \varepsilon^2}{k};$$

$$P_в = -\frac{g_i}{\sigma_в \rho}\frac{\partial \rho}{\partial x_i};$$

$$\tau_{ij} = \mu_т\left(\frac{\partial u_i}{\partial x_j} + \frac{\partial u_j}{\partial x_i} - \frac{2}{3}\frac{\partial u_k}{\partial x_k}\delta_{ij}\right) - \frac{2}{3}\rho k \delta_{ij},$$

g_i – gravitational acceleration component along the x_i;

$$f_1 = 1 + \left(\frac{0{,}05}{f_\mu}\right)^3; \quad f_2 = 1 - \exp\left(-R_т^2\right);$$

$C_в = 1$ при $P_в > 0$, $C_в = 0$ при $P_в \le 0$;

$$\sigma_в = 0{,}9; \quad C_{\varepsilon 1} = 1{,}44; \quad C_{\varepsilon 2} = 1{,}92; \quad \sigma_\varepsilon = 1{,}3; \quad \sigma_k = 1.$$

In order to simulate laminar flows, the system of equations k-ε model is modified, namely, it is assumed that $\mu_т = 0$ and $k = 0$. The transition of laminar flow into turbulent flow and turbulent flow into laminar flow is simulated with the function f_μ [6].

Numerous publications indicate that using the equations of k-ε model it is possible to describe a wide class of turbulent flows quite adequately. However, for example, when describing swirling flows, the model gives incorrect results [7]. It should be noted that equations of k-ε model are valid only for developed turbulent flow. In the vicinity of solid surfaces, special consideration of setting of boundary conditions for k, ε and tangential component of velocity vector near the wall is required. In a number of studies dedicated to simulation of turbulent flows in plasma generators in order to eliminate drawbacks inherent to k-ε model, it was replaced by other models in the near-wall region. For example, in the work [8], Prandtl model with subsequent cross-linking of models was used for this purpose. This approach, however, does not guarantee quality results. For complex flows, cross-linking the Prandtl mixing length model and the k-ε model becomes problematic.

It should be noted that in view of the introduced design criterion, it becomes particularly important to simulate flows in the near-wall region of the cathode assembly. Due to the fact that the viscous gas velocity near the wall is low, this is where active gases should be expected to break through into the cathode sheath. Therefore, the application of the standard k-ε model for selecting the flow geometry of cathode assemblies and the modes of protective gas supply requires justification.

Further modifications of the standard k-ε model allowed to some extent eliminate its defects. Among these modifications, the RNG k-ε model has to be highlighted the most. The RNG k-ε model has been developed on the basis of strict statistical methods (renormalization group theory). The main differences between RNG k-ε and the standard k-ε model are as follows. In the standard model the values of constants are obtained on the basis of its fitting to experimental results. The RNG model gives analytical expressions for the constants. This is especially significant with respect to the constants of the equation for ε as the way of its derivation and the values of the constants have been repeatedly analysed and criticised [3].

While the standard k-ε model is a high Reynolds model, the RNG theory provides an analytically derived differential effective viscosity formula which is more suitable for calculating low Reynolds flows which are most common in industrial plasma equipment.

These features make the RNG k-ε model more accurate and reliable for a wide range of turbulent flows, in particular when simulating the flow of gases in electric arc plasma generators. The k-ω turbulence model uses the turbulence frequency equation ω instead of the energy dissipation equation. This equation has significant advantages near the wall surface and accurately predicts the scale of turbulence in flows with large pressure gradients. Moreover, this model has a very simple low Reynolds formulation.

The expression for turbulent viscosity using the k-ω model is written as [9]:

$$\mu_т = \frac{\rho k}{\omega}. \qquad (10)$$

Two additional equations are used to determine the turbulence kinetic energy and turbulence frequency:

$$\frac{\partial \rho k}{\partial t} + \frac{\partial}{\partial x_i}(\rho v_i k) = \tau_{ij}\frac{\partial v_i}{\partial x_j} - \beta^* \rho \omega k + \frac{\partial}{\partial x_i}\left((\mu_л + \sigma_{k1}\mu_т)\frac{\partial k}{\partial x_i}\right), \quad (11)$$

$$\frac{\partial \rho \omega}{\partial t} + \frac{\partial}{\partial x_i}(\rho v_i \omega) = \frac{\gamma_1}{\nu_т}\tau_{ij}\frac{\partial v_i}{\partial x_j} - \beta_1 \rho \omega^2 + \frac{\partial}{\partial x_i}\left((\mu_л + \sigma_{\omega 1}\mu_т)\frac{\partial \omega}{\partial x_i}\right), \quad (12)$$

where $\beta = 3/40$; $\beta^* = 9/100$; $\sigma_{k1} = 1/2$; $\sigma_{\omega 1} = 1/2$.

The advantage of this model over various formulations of the k-ε model is a better fit of simulation results to experimental data in the near-wall region, which has been repeatedly confirmed by various researchers in numerical experiments. At the same time, its use for simulation of turbulent flows outside the boundary layer may lead to large errors.

In the work [10], an approach was proposed which allowed combining k-ε and k-ω models of turbulence, using each of them where it's the most accurate: k-ε - in the region of developed turbulence and k-ω - in the near-wall regions.

For this purpose, the equations of the k-ε model were rewritten in an equivalent k-ω formulation:

$$\frac{\partial \rho k}{\partial t} + \frac{\partial}{\partial x_i}(\rho v_i k) = \tau_{ij}\frac{\partial v_i}{\partial x_j} - \beta^* \rho \omega k + \frac{\partial}{\partial x_i}\left((\mu_л + \sigma_{k1}\mu_т)\frac{\partial k}{\partial x_i}\right),$$

$$\frac{\partial \rho \omega}{\partial t} + \frac{\partial}{\partial x_i}(\rho v_i \omega) = \frac{\gamma_2}{\nu_т}\tau_{ij}\frac{\partial v_i}{\partial x_j} - \beta_2 \rho \omega^2 + \frac{\partial}{\partial x_i}\left((\mu_л + \sigma_{\omega 2}\mu_т)\frac{\partial \omega}{\partial x_i}\right) +$$

$$+ 2\rho\sigma_{\omega 2}\frac{1}{\omega}\frac{\partial k}{\partial x_j}\frac{\partial \omega}{\partial x_j}.$$

The equations (13) of the standard k-ω model were then multiplied by the F_1 function and the transformed equations of the k-ε model were multiplied by the $1\text{-}F_1$ function. This function plays the role of a switch between the models and is constructed to be equal to one near the wall and 0 – away from the surface.

Adding these expressions results in the basic formulation of the combined model (14).
All empirical constants Φ_1 of the standard k-ω model, Φ_2 of the transformed k-ε model and Φ of the combined model are connected by a relation (15).

In addition to combining k-ε and k-ω models in the model proposed by Menter, called the SST (shear-stress transport) model, another fundamental innovation has been introduced. An important advantage of the Reynolds full-stress transport models compared to the two-parameter turbulence models studied is the adequate accounting of the turbulent shear-stress transport.

$$\frac{\partial \rho k}{\partial t}+\frac{\partial}{\partial x_i}\left(\rho v_i k\right)=\tau_{ij}\frac{\partial v_i}{\partial x_j}-\beta^{*}\rho\omega k+\frac{\partial}{\partial x_i}\left(\left(\mu_{л}+\sigma_k\mu_{т}\right)\frac{\partial k}{\partial x_i}\right),$$

$$\frac{\partial \rho\omega}{\partial t}+\frac{\partial}{\partial x_i}\left(\rho v_i \omega\right)=\frac{\gamma}{\nu_{т}}\tau_{ij}\frac{\partial v_i}{\partial x_j}-\beta\rho\omega^{2}+\frac{\partial}{\partial x_i}\left(\left(\mu_{л}+\sigma_{\omega}\mu_{т}\right)\frac{\partial \omega}{\partial x_i}\right)+$$

$$+2\rho(1-F_1)\sigma_{\omega 2}\frac{1}{\omega}\frac{\partial k}{\partial x_j}\frac{\partial \omega}{\partial x_j}.$$

$$\Phi = \Phi_1 F_1 + (1 - F_1)\,\Phi_2. \tag{15}$$

It has been suggested by Mentor that the F_1 function should be chosen in the form of a stable computation:

$$F_1 = \tanh(arg_1^4), \tag{16}$$

where

$$\arg_1 = \min\left[\max\left(\frac{\sqrt{k}}{0.09\omega y};\frac{500\nu}{y^2\omega}\right);\frac{4\rho\sigma_{\omega 2}k}{CD_{k\omega}y^2}\right];$$

y – distance to the nearest wall;

$$CD_{k\omega}=\max\left(2\rho\sigma_{\omega 2}\frac{1}{\omega}\frac{\partial k}{\partial x_j}\frac{\partial \omega}{\partial x_j},10^{-20}\right).$$

More often, the swirling nature of the plasma gas supply has to be taken into account when modelling flows for plasma equipment.

However, most authors, when applying RANS models of turbulence, ignore the fact that they are not suitable for describing swirling flows. It is well known [11] that curvature of current lines and flow rotation have a significant effect on the characteristics of turbulence and can lead to both its significant intensification and suppression. These effects are, in principle, automatically described within the framework of Reynolds stress transport models. In the framework of linear models, however, special corrections must be introduced in order to take them into account. The most successful of such corrections seems to be the Spalart-Shur correction [12], which takes into account the single nature of curvature effects of current and rotation lines and is applicable, generally speaking, to any linear models. However, a specific calibration of the correction called "Rotation-Curvature correction" (RC) has been done for SA and SST model.

In the SARC model, the generative component P^{ν} is modified by multiplying by an empirical function:

$$f_{r1}=\frac{2r^{*}\cdot\left(1+C_{r1}\right)}{1+r^{*}}\left(1-C_{r3}arctg\left(C_{r2}\tilde{r}\right)\right)-C_{r1}. \tag{17}$$

The function (17) depends on two parameters r^* and , which are measures of curvature of current and rotation lines.

The results obtained in the works [1, 2] in the framework of the gas dynamic approach showed satisfactory agreement with the experimental data (given in Fig. 2), which allowed to conclude that the SST, RNG k-ε models meet the requirements for turbulence models when describing the character of flow in the gas discharge channel of plasma equipment. However, this conclusion is based on results obtained without considering the thermal effects of the electric arc. In order to adequately describe the complex turbulent nature of the flow with the presence of tear zones and recirculation flows associated with the movement of the electric arc roots, a more reasonable choice of turbulence model is needed.

The models considered above do not meet the requirements and are not applicable to the calculation of such complex flows.

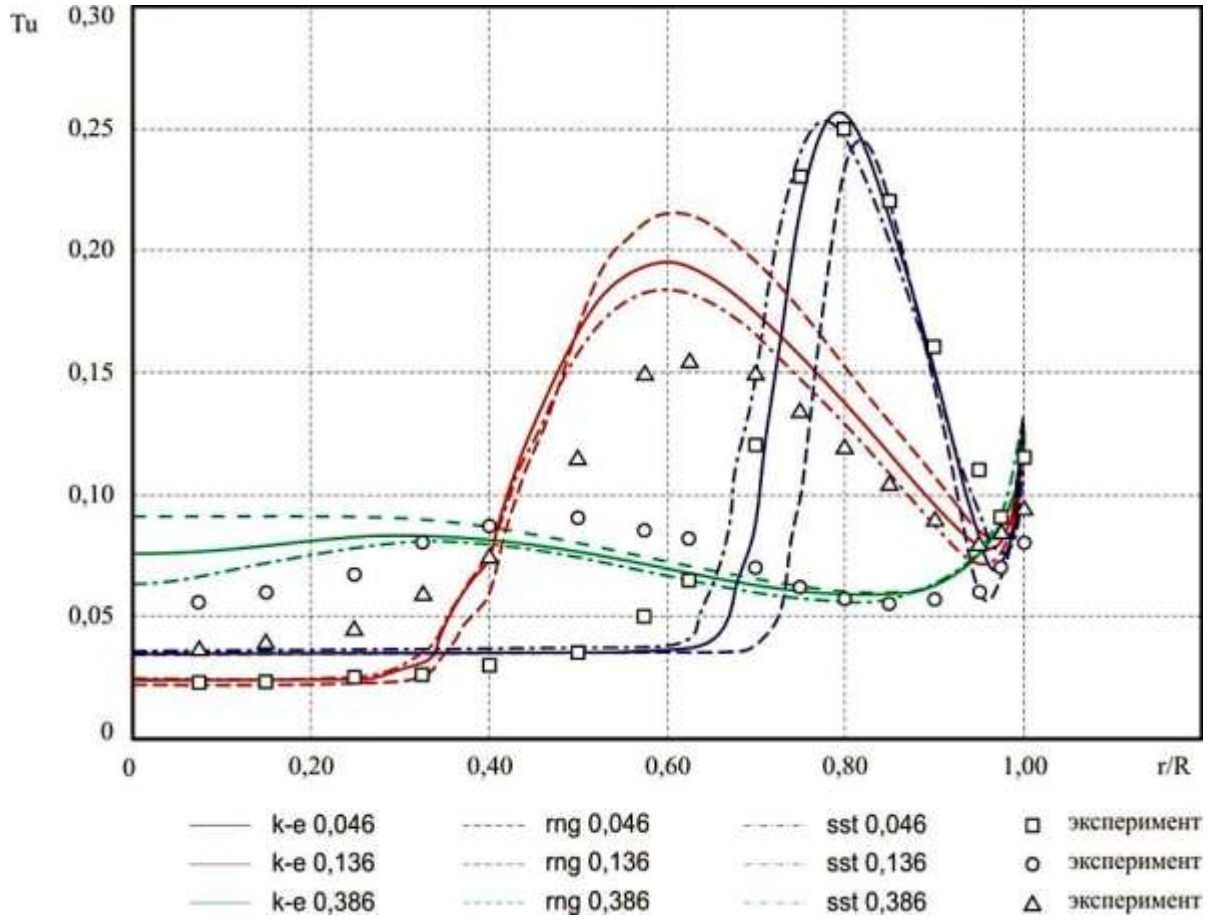


Figure 2 – Turbulence intensity for a swirling flow

LES model. The equations underlying LES can be derived from the Navier-Stokes equations by representing all variables as a sum of the large- and small-scale components and applying a filtration procedure to the resulting equations. The final form of the basic LES equations for compressible gas:

$$\begin{cases} \dfrac{\partial \rho}{\partial t} + \nabla \cdot (\rho \vec{u}), \\ \dfrac{\partial (\rho \vec{u})}{\partial t} + \nabla \cdot (\rho \vec{u} \vec{u}) = -\nabla p + \nabla \cdot (\tau_m + \tau_{SGS}), \\ \dfrac{\partial (\rho E)}{\partial t} + \nabla \cdot (\rho \vec{u} H) = \nabla \cdot \left[\vec{u} \cdot (\tau_m + \tau_{SGS}) + (\vec{q}_m + \vec{q}_{SGS}) \right]. \end{cases} \quad (18)$$

The only formal difference between equations (18) and Reynolds equations is a difference in notation of additional summand appearing in right parts of equations of motion and energy as a result of spatial filtration of convective terms of Navier-Stokes equations (LES) and their time averaging (RANS): in LES equations these terms have index “SGS” (sub-grid), and in RANS equations – index “t” (turbulent). However, behind these different designations, there is a fundamentally different physical content of LES and RANS approaches to describing turbulent flows, which is directly manifested at the stage of system closure (18), i.e. when building turbulence models (as well as simulated terms themselves), these models are called sub-grid.

Thus, additional (containing Reynolds stresses) RANS terms describe the effect of all turbulent inhomogeneities on the averaged solution, while similar terms of LES equations (“sub-grid” stresses) describe the effect of only relatively small (smaller than filter size Δ) vortices on the time-dependent solution of filtered equations. In other words, within the LES framework, vortex structures with sizes larger than the filter size are resolved “exactly”, and only smaller vortex structures are simulated. To emphasise this, turbulence models for LES are referred to as “sub-grid” models.

From the above description, it becomes clear that if the filter size corresponds to a wave number k_Δ lying in the universal (“inertial”) region of the turbulence energy spectrum, that is, if $k_I < k_\Delta < k_d$, then only relatively universal (independent of specific geometry and boundary conditions) vortices are subject to simulation. As a result, the role of the undercut model in LES is reduced to ensuring the correct cascading rate of turbulence energy transfer from large to small vortices within the inertial wave number interval or, in other words, the correct dissipation rate of the smallest “allowed” vortices.

This is the fundamental advantage of the LES over the RANS approach, which requires simulation of all, including large energy-containing vortices that do not meet any universal law. From a practical point of view, this advantage means a significant reduction in the requirements for subset models for LES compared to turbulence models to close the RANS equations. In particular, experience with LES has convincingly demonstrated that if the condition $k_I < k_\Delta < k_d$ is fulfilled, it provides high accuracy in calculating not only the averaged and basic statistical, but also the pulsation characteristics of turbulence, even when using the simplest sub-grid models.

Like the models for RANS, sub-grid models are generally based on the use of generalised Boussinesq hypothesis and Fourier law:

$$\tau_{SGS} = 2\mu_{SGS}\left(S - \frac{1}{3}(\nabla \cdot \vec{u})I\right) + \frac{2}{3}k_{SGS}I, \vec{q}_{SGS} = -\lambda_{SGS}\nabla T. \quad (19)$$

However, this is where the similarities between the two approaches end, as the relations used to determine the sub-grid viscosity are fundamentally different from the turbulent viscosity models for the Reynolds equations.

The natural price to pay for the described advantages of LES is that it requires incomparably more computational resources than RANS. This is due to the need, as in the case of DNS, to perform three-dimensional non-stationary calculations on rather small grids, even in cases where the purpose of calculation is to determine only parameters of the averaged flow. On the other hand, for obvious reasons (the fine-scale part of the spectrum is simulated rather than calculated "exactly"), the resources required to implement LES turn out to be much smaller than for DNS. Thus, for the calculation of turbulence away from solid walls, the number of grid cells required for LES increases with increasing Reynolds number much slower than for DNS: proportional to $Re^{0.4}$ rather than $Re^{2.25}$. However, near walls, where even energy-carrying vortices have very small sizes, the grid requirements for LES become significantly more stringent and approach the same requirements for DNS: number of cells required for LES of such currents is proportional to $Re^{1.8.}$

As an illustration, Fig. 3 shows dependence of the Reynolds number and number of grid cells that should be in the inner and outer regions of the boundary layer on the plate when calculating it in the framework of LES [13]. The figure shows, in particular, that for $Re = 10^6$ the total number of cells is $\sim 10^{8.5}$, where 99% of which are in the inner part of the boundary layer.

DES and SAS turbulence models. As noted above, DES method has been proposed as an alternative to RANS and LES methods for the calculation of near wall flows with extensive tearing zones, for which RANS models are unable to provide acceptable accuracy and LES requires excessively large computational resources, thus delaying its wide practical use. It was taken into account that the lion's share of the computational cost of LES is connected with the calculation of the near-wall part of the coupled boundary layers, populated by energy-carrying vortices of small sizes, and that the calculation of just such flows with RANS is rather reliable and economical. This naturally led the DES authors to the idea of a combined RANS-LES model which would combine the best qualities of both methods, namely the reliability and computational efficiency of RANS in coupled boundary layers with the clear physics, high accuracy and acceptable computational cost of LES away from the walls (see Figure 4).

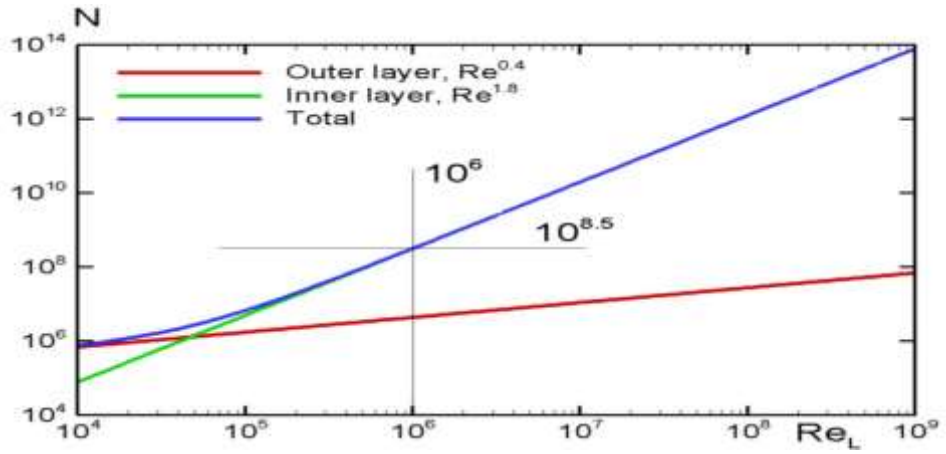


Figure 3 – Dependence of the number of grid cells in the inner and outer regions of the boundary

layer on a flat plate and the total number of grid cells needed for LES of a given flow on Reynolds number

This very combination of RANS and LES proposed in 1997 and was called the Detached-Eddy Simulation method. This name underlines the fundamental difference between DES and LES. The difference is that DES does not "exactly" compute all energy-carrying vortices but only "detached" vortices that populate the detached zones, while the vortices populating the regions of the attached boundary layers are described by conventional semiempirical RANS models. Another important feature of DES is that this approach uses the same "basic" turbulence model in RANS and LES regions, which functions as a RANS model inside the wall boundary layer and as its sub - Grid Scale or SGS counterpart away from the solid walls. The first version of DES [14] used the SA model as such a base model, but later modifications of DES based on other RANS models, in particular the SST model [15], have been proposed.

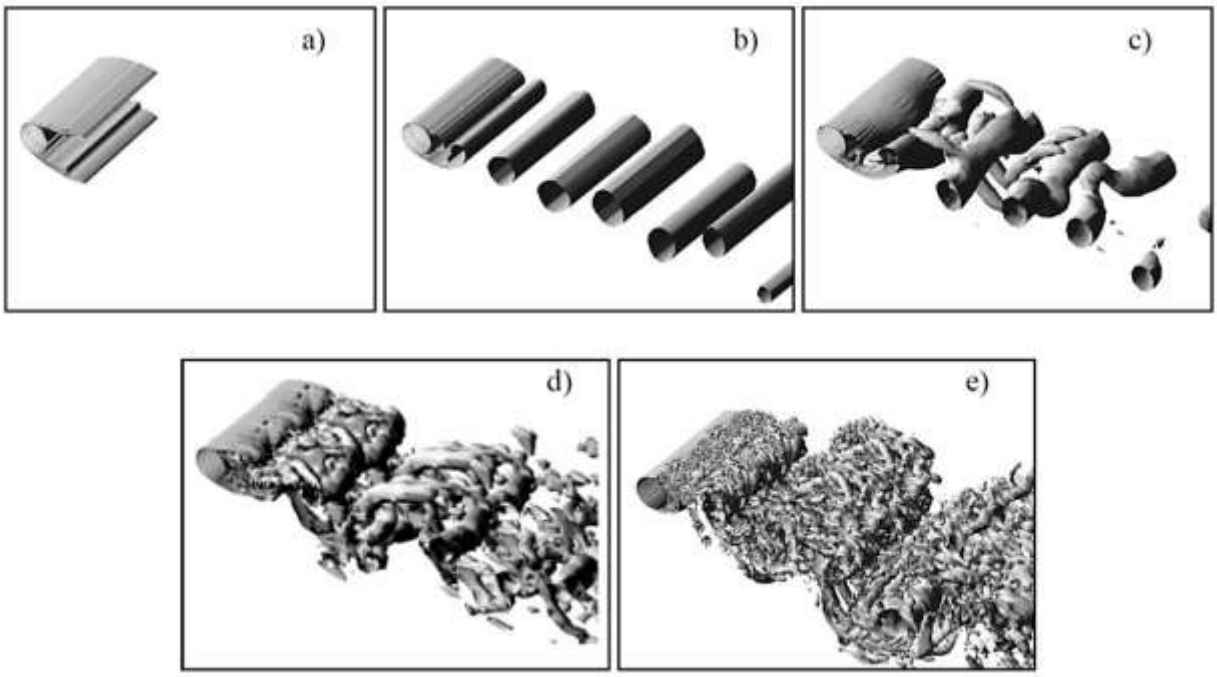


Figure 4 – Isosurface of the parameter λ_2 (modulus of the second eigenvalue of the velocity gradient tensor) from the calculations of the precritical flow around a circular cylinder performed within different turbulence simulating approaches:

(a) Two-dimensional steady Reynolds equations, SA model;
(b) Two-dimensional unsteady Reynolds equations, SA model;
(c) Three-dimensional unsteady Reynolds equations, SA model;
(d) SA DES on a coarse grid;
(e) SA DES on a fine grid.

Figure 4 gives an overview of the possibilities offered by DES compared to other approaches to simulate detached flows, using the example of a circular cylinder flowing at Reynolds number Re = 1,4·1, corresponding to the subcritical flow regime (laminar boundary layer detachment and transition to turbulence in the detached mixing layer). It shows, in particular, that when calculating this flow in the framework of the stationary two-dimensional Reynolds equations (2D RANS), the velocity field turns out to be symmetric with respect to the geometric symmetry plane of the cylinder.

When the same problem is solved within non-stationary two-dimensional Reynolds equations (2D URANS), a two-dimensional Karman vortex street is formed in the cylinder trace, while using three-dimensional equations (3D RANS), longitudinal vortex structures are imposed on it. However, for all the principal differences noted, none of these three approaches allow such important parameters of the averaged flow as the cylinder drag and the length of the recirculation zone in its wake to be predicted with an acceptable degree of accuracy.

In contrast, when using DES, all these parameters can be calculated with fairly high accuracy, even on relatively coarse grids (on the order of half a million cells in this case), and as the grid is refined, the calculation error decreases and in the limit tends to zero (DES converts to DNS).

The idea behind the DES method is quite simple and is based on the fact that the RANS and LES equations share a common form. Furthermore, it is assumed that the RANS model, from which the DES model is derived, can be converted into a sub-grid model for LES by replacing the linear turbulence scale l_{RANS}, explicit or implicit in all RANS models, by a sub-grid scale $l = C\Delta$.Then introducing the hybrid scale:

$$l_{DES} = \min\{l_{RANS}, C_{DES}\Delta\},$$

where C_{DES} is an additional model constant similar to that of Smagorinsky, we obtain a DES model which, depending on the ratio of the linear scales RANS and LES, l_{RANS} and C_{DES}, functions either as a basic RANS model or as its sub-grid version.

An important feature of DES is also the fact that it uses the maximum of the three grid steps at the considered flow point as the characteristic “filter” size: $max\{\Delta_x, \Delta_y, \Delta_z\}$.

Taking into account the strong anisotropy of grids used in the domain of the coupled boundary layer ($\Delta_x \approx \Delta_y >> \Delta_z$ – see Fig. 3), this definition of the linear sub-grid scale for LES seems physically more correct than, for example, the most common definition $\Delta = (\Delta_x, \Delta_y, \Delta_z)^{1/3}$.

The greatest disadvantage of the DES turbulence model is the possibility of incorrect determination of the detachment point of the near-wall flow, which is associated with the DES switching to the LES mode inside the boundary layer due to the finite-element grid step refinement in the directions tangent to the streamlined surface.

For proper operation of DES it is necessary for the whole boundary layer to be in the RANS domain while DES must fulfill the inequality $\Delta_{II} > \delta$, where Δ_{II} is grid steps in the directions parallel to the wall, δ is the thickness of the boundary layer.

In the works [10, 16, 17], the SAS (Scale-Adaptive Simulation) turbulence models have been proposed as an alternative to using DES, which is an improvement of the non-stationary RANS method and allows to obtain reliable data for flow pulsations.

The corresponding equations of the SAS turbulence model can be represented as:

$$\frac{\partial k}{\partial t}+\frac{\partial}{\partial x_j}(\vec{u}_j k)=\frac{\partial}{\partial x_j}\left[\left(\nu+\frac{\nu_t}{\sigma_k}\right)\frac{\partial k}{\partial x_j}\right]+P_k-\beta\cdot k\omega,$$

$$\frac{\partial \omega}{\partial t}+\frac{\partial}{\partial x_j}(\vec{u}_j \omega)=\frac{\partial}{\partial x_j}\left[\left(\nu+\frac{\nu_t}{\sigma_\omega}\right)\frac{\partial \omega}{\partial x_j}\right]-\beta\omega^2+C_\omega+aS^2+Q_{sas}, \quad (20)$$

where

$$Q_{sas}=\max\left[\varsigma_2 kS^2\left(\frac{L}{L_{vk}}\right)^2-C\cdot\frac{2k}{\sigma_\Phi}\max\left(\frac{|\nabla\omega|^2}{\omega^2},\frac{|\nabla k|^2}{k^2}\right),0\right].$$

Unlike the traditional URANS models, which only allow for large-scale turbulent structures, the SAS model adapts dynamically to scales already solved and allows for capturing the development of turbulent structures in individual flow regions.

The SAS concept is based on the introduction of the Karman length into the turbulence scale equation (Q_{sas} term in system (20). The information obtained with this variable allows the SAS model to dynamically adapt to the characteristics of structures that have already been solved by URANS. This leads to the fact that in areas of unsteady flow the model works similarly to the large vortex method. At the same time, in areas where the flow is stationary, the SAS model behaves similarly to the RANS models. As can be seen from (20), the model is based on the SST equations of turbulence model, which is well-proven for a wide range of problems, including gas-dynamic design of cathode assemblies.

The advantages of the SAS-SST turbulence model are obvious: it is more technologically advanced than the DES method, the dynamic adaptation of the model to the computational grid size eliminates the possibility of false detachment flows related to the quality of the finite element grid.

The model is less demanding in terms of grid quality and number of grid elements than the DES and LES models, both in near-wall areas as well as in areas with developed flow. As the number of grid nodes increases, the accuracy of the result obtained increases, and the model behaves similarly to the LES model of turbulence.

Current tabular and reference data on the transfer properties and thermodynamic properties of gases and their mixtures cover limited temperature and pressure ranges. In Order to obtain these properties in a given temperature range (300...30000 K), it is necessary to calculate transfer equations and transfer coefficients included in these equations – viscosity, thermal conductivity, electrical conductivity, coefficients characterising the diffusion and thermodiffusion properties of the components. There are methods for calculating transfer coefficients based on higher approximations of Chapman-Enskog method in a wide range of pressure and temperature taking into account chemical reactions and ionization [18, 19]. The main assumptions used in the method are listed below:

- the gas mixture is treated as a mixture of ideal dilute gases, i.e. the following relations take place: $d^* << l^* << L^*$, where d^* is the average particle size, l^* is the average free path length, L^* is the variation scale of macroscopic characteristics (characteristic flow size);
- -collisions of all particles are binary, distribution functions for all particles f_k *(k = 1,...,N)*

deviate little from the Maxwell equilibrium $f_k^{(0)}$, i.e. $f_k = f_k^{(0)}(1 + \varphi_k^{(1)})$, and Boltzmann equations can be solved by the Chapman-Enskog method with expansion of corrections to distribution functions $\varphi_k^{(1)}$ by Sonin polynomials;

- gas and plasma are assumed to be thermally equilibrium, i.e. all degrees of freedom of atoms, molecules, ions and electrons (translational, rotational, vibrational, electronic) have the same temperature T.
- plasma is ideal;
- external magnetic field is absent or small and does not affect the transport properties of plasma;
- the influence of chemical reactions and ionization on the transfer coefficients can be neglected, i.e. "chemical" inelastic collisions disturbing the equilibrium distribution cannot be taken into account. This corresponds to the assumption that characteristic times of all reactions are large in comparison with average free paths of particles and reaction rates are much smaller than the rate of establishment of Maxwell equilibrium due to elastic collisions.

Parameters of a given model of interaction potential or scattering cross-section can be obtained (reconstructed) by means of experimental beam scattering studies; for example, scattering cross-sections for electron-atom and electron-molecule interactions are obtained in [20]. Other experimental data are also used: study of the ion mobility in the electric field, spectroscopic data, etc.

If for the required type of interaction of complex particles (molecules, ions) there are no reliable experimental and theoretical data, the interaction potential can be constructed with the help of empirical methods, for example, the method of atom-atom potentials [21], which uses the sum of interaction potentials of separate atoms, composing a complex particle.

In the works [22, 23] available experimental and theoretical data on collision cross-sections and interaction potentials are analysed, the most reliable data and models for all kinds of interactions are chosen and collision integrals of all necessary orders are calculated, if there were no data available for them in literature.

Models of interaction potentials and formulas approximating the collision integrals for main types of interactions are presented in the work [24].

The results of numerical calculation of the transfer coefficients for air and argon are given in Figures 5-8 (here the dashed lines correspond to air and the solid lines to argon).

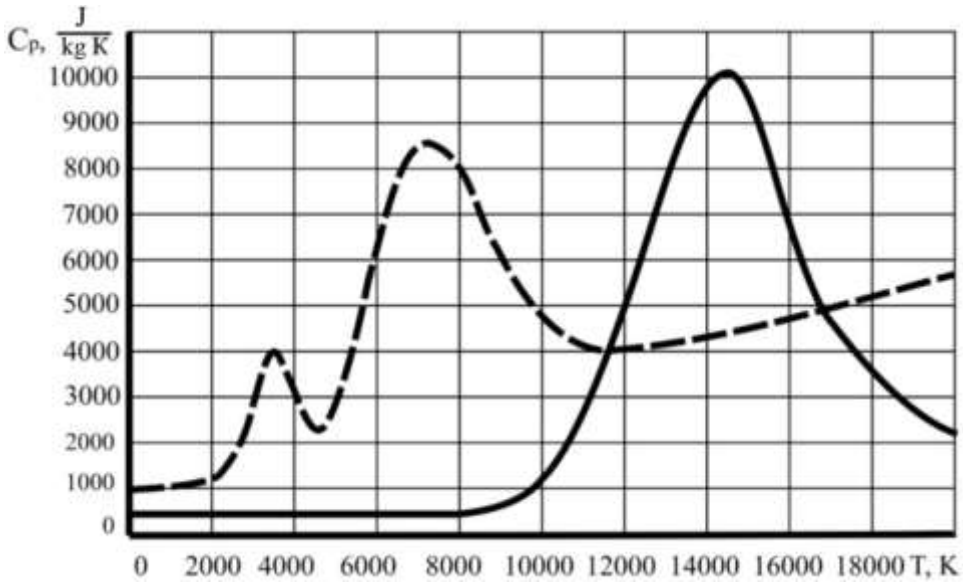


Figure 5 – Dependencies of component heat capacity on temperature

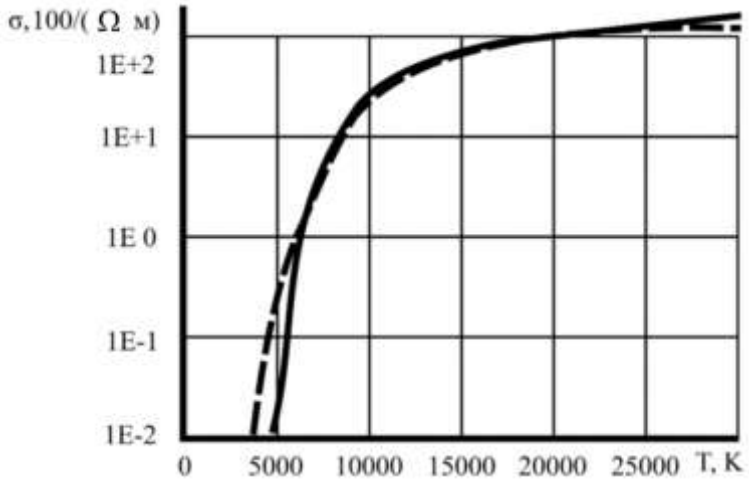


Figure 6 – Dependencies of component conductivity on temperature

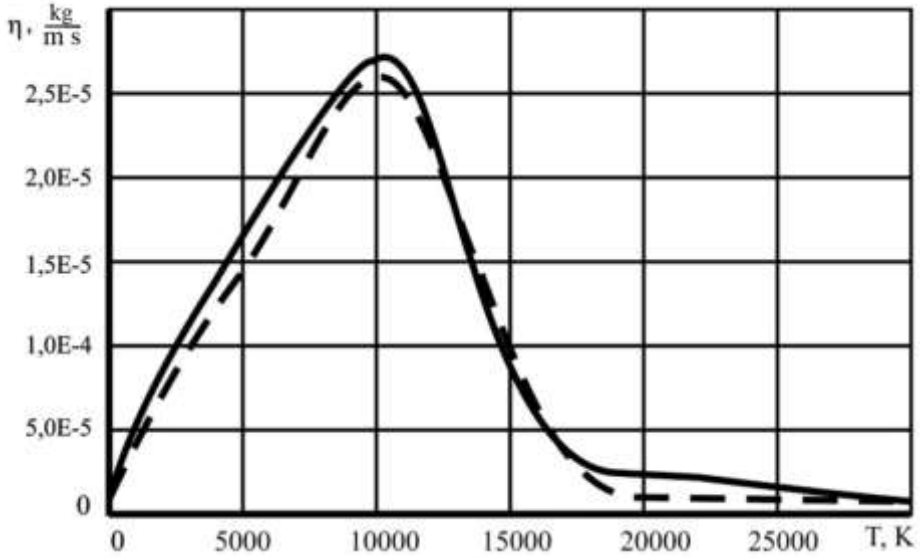


Figure 7 – Dependencies of component thermal conductivity on temperature

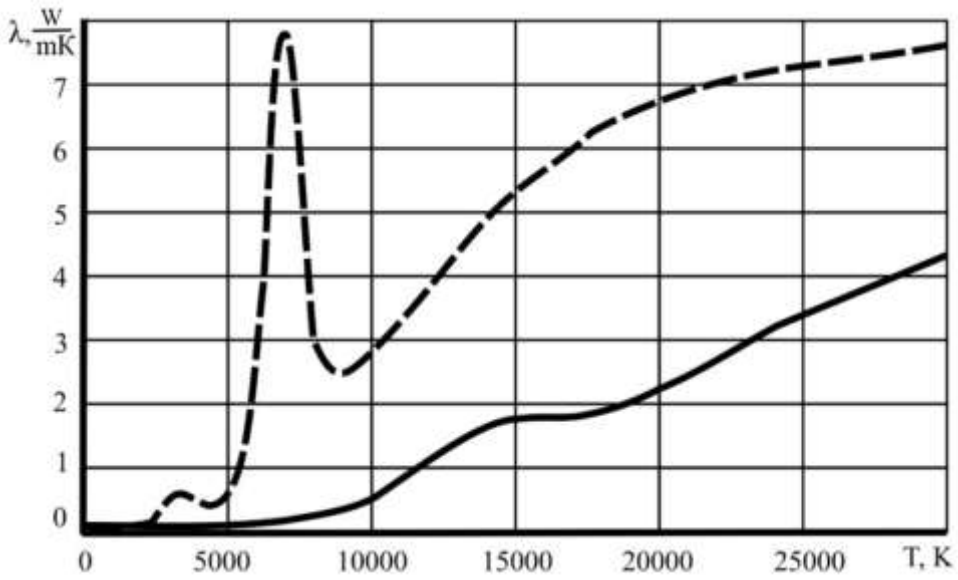


Figure 8 – Dependencies of component thermal conductivity on temperature

Results of the study and their discussion

The results of numerical experiments on the test problem (Fig. 9) using the above mathematical dependencies (2) - (20) for models with cold gas purging show good agreement with experimental data only for the initial operating stages of the plasma equipment.

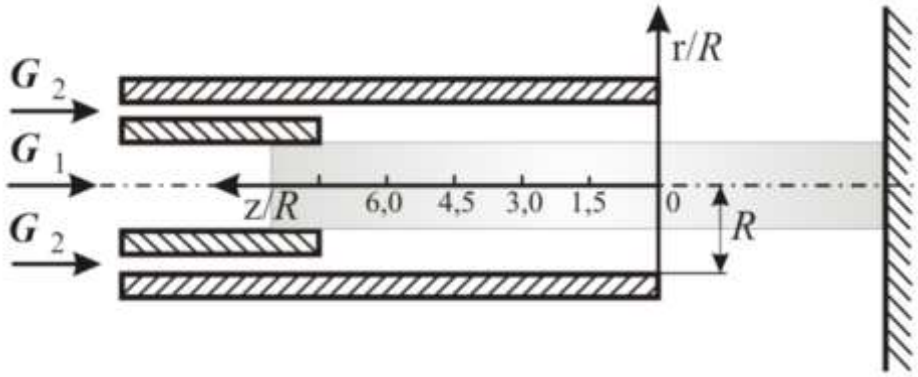


Figure 9 - Schematic diagram of the test problem

However, in operating modes, the presence of an intense heat source (electric arc) significantly affects both the flow pattern and the properties of the gas mixture components.

In the work [25], an approach based on representation of electric arc as a volumetric energy source was proposed to determine the parameters of gas dynamic protection. The following problem was considered: plasma-forming gas (argon) is fed through hollow cathode with G_1 flow rate and through coaxial gap with G_2 flow rate between cathode and channel wall. The gas feeding through the cathode cavity is axial, through the gap – with the possibility of swirling.

The arc (shaded in the figure) burns between the hollow cathode and a flat surface perpendicular to the axis of the cathode assembly.

In the test problem, the heat transfers between the gas flow and the walls were not considered. The walls of the hollow cathode and the heated surface were considered adiabatic and the condition of constant temperature was set for the channel walls of the cathode assembly. The gas inside the cathode assembly was simulated as an ideal two-component mixture (air + argon). Nonlinear dependence of component characteristics on temperature was taken into account, and the intensity of the volume source was determined taking into account Joule heating and arc radiation.

In the works [25, 26] the results on determining the atmosphere composition in the cathode assembly channel, obtained according to the results of cold blows and taking into account the arc influence on the flow parameters and properties of gas mixture components were compared. At the same geometrical parameters of the problem and noble gas flow rates, the results differed significantly. The partial pressure of air near the cathode for the problem taking into account the influence of arc was more than 60 Pa (Fig. 10), which exceeds the critical level for all known emission materials.

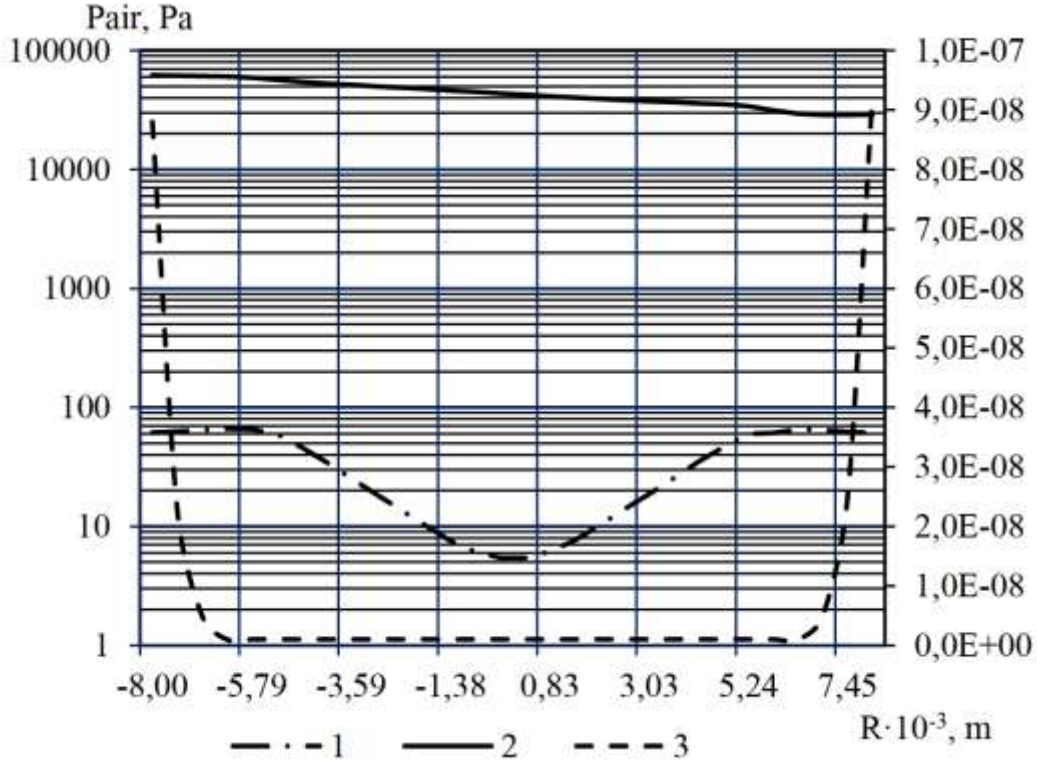
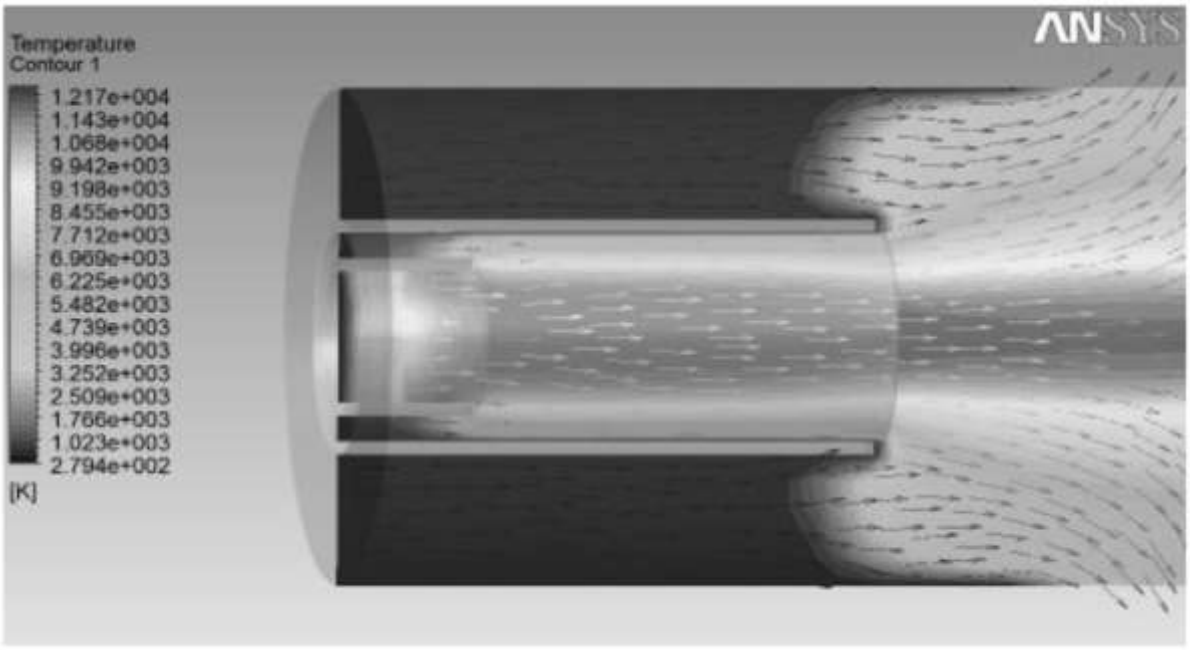


Figure 10 – Partial air pressure at the cathode cut-off
1 – gas-dynamic approach with consideration of thermal impact of electric arc;
2 – proposed approach with consideration of the magneto-electric component (left ordinate scale);
3 – gas-dynamic approach

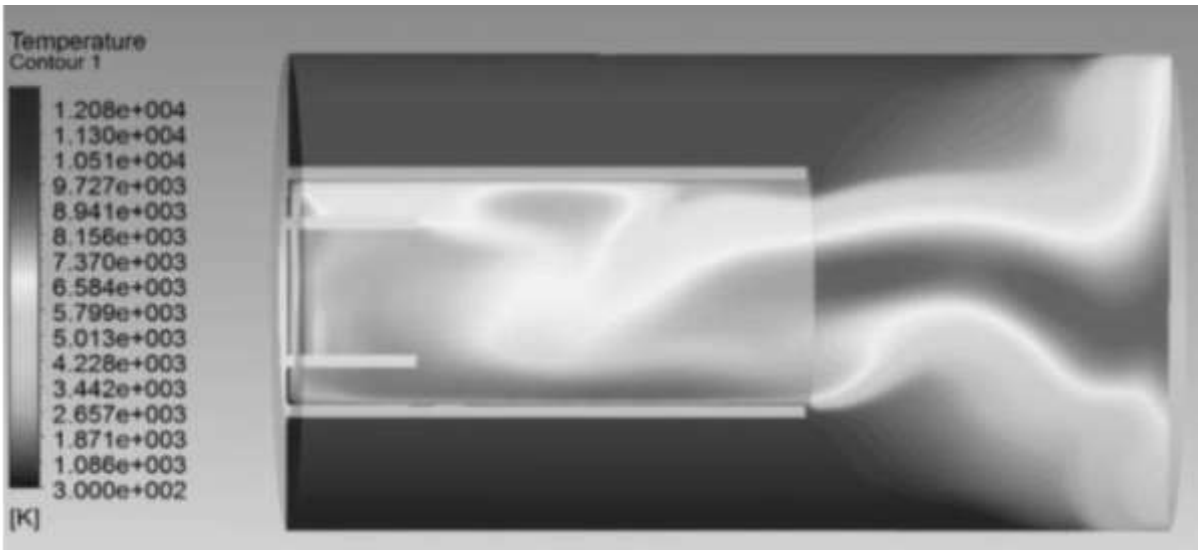
Recently, another approach to simulating flows in plasma generators, based on the application of the MGD approximation, has become increasingly popular. The popularity of this approach is largely due to the introduction of MGD flow simulation capabilities in recent versions of commercial CFD packages (ANSYS CFX, FLUENT, etc.). In the work [27], a comparative analysis of different approaches to simulation processes in the electric arc equipment has been performed.

The results obtained for similar geometry within magnetogasdynamic approach showed significant difference in partial pressure values both for the case of cold blows and for the case with electric arc simulation.

Fig. 10 shows that the partial pressure for the case of MGD simulation makes $3...6 \cdot 10^4$ Pa, while for the gas-dynamic approach the maximum pressure near the cathode makes only 60 Pa. Such difference in the results is explained, first of all, by non-uniformity of temperature field inside the gas-discharge channel (see Fig. 11).



a



b

Figure 11 – Temperature distribution for the test problem within gas-dynamic (a) and magnetogasodynamic approaches (b)

The gas dynamic approach considers only one mechanism for oxygen-containing gases to penetrate into the cathode space – counter diffusion along the channel wall in the boundary layer. In the case of MGD problem the main mechanism of penetration of oxygen-containing gases is their penetration into the reverse flow area resulting from chaotic movement and bending of the electric arc caused by the interaction of the arc itself with the cold gas flow and the action of electromagnetic Lorentz force.

As a test case in this paper, the following problem was considered: a cylindrical tungsten cathode has a length of 30 mm and a diameter of 3.2 mm. The cathode is tapered at an angle of 60 degrees and has a flat pad of 0.2mm diameter at the end. The flat copper anode is 5 mm from the end of the cathode. In calculations, the flow rate of protective gas (argon) through an annular slot of 5mm, 10l/min, which corresponds to a speed of 1.3 m/s, is set. The temperature at the outer end of the cathode and at the lower surface of the anode is fixed at 300 K.

An adiabatic wall condition is set on the side surface of the anode. The ambient temperature is 300K. When simulating the multi-component composition of the gas medium (air-argon) has been taken into account.

As the initial conditions in the area between the cathode and anode, a zone with the initial temperature of about 7000-1200 K is set to impart the initial conductivity to the gas.

Based on the recommendations of the work [28], the cell sizes for the electrode sheathes of the finite-element model, hexagonal grid were chosen – 0.01 cm and 0.04 cm which corresponded to the ratio D_e / W, where D_e – the electron diffusion coefficient and W – the electron drift velocity. These values of wall element sizes provide the most stable computational process.

Convergence control of the solution was carried out based on the condition:

$$\max\left|\frac{\varphi(M)-\varphi^{*}(M)}{\varphi(M)}\right| \le \varepsilon \quad ,$$

where φ is the value of the variable in the assembly M of the control volume obtained in the previous iteration of the solution, and φ* is the value in this iteration, ε – 0.005.

Fig. 12 shows the picture of isotherms and flow obtained from the simulation, the maximum temperature was 21800 K and maximum on-axis velocity of cathode jet was 275 m/s which is in satisfactory agreement with the results of other authors. In Fig. 13 the dependence of the temperature on the distance to the cathode axis is shown both experimentally and numerically.

The discrepancy with the experimental data was not more than 6% for the temperature and 3% for the maximum velocity.

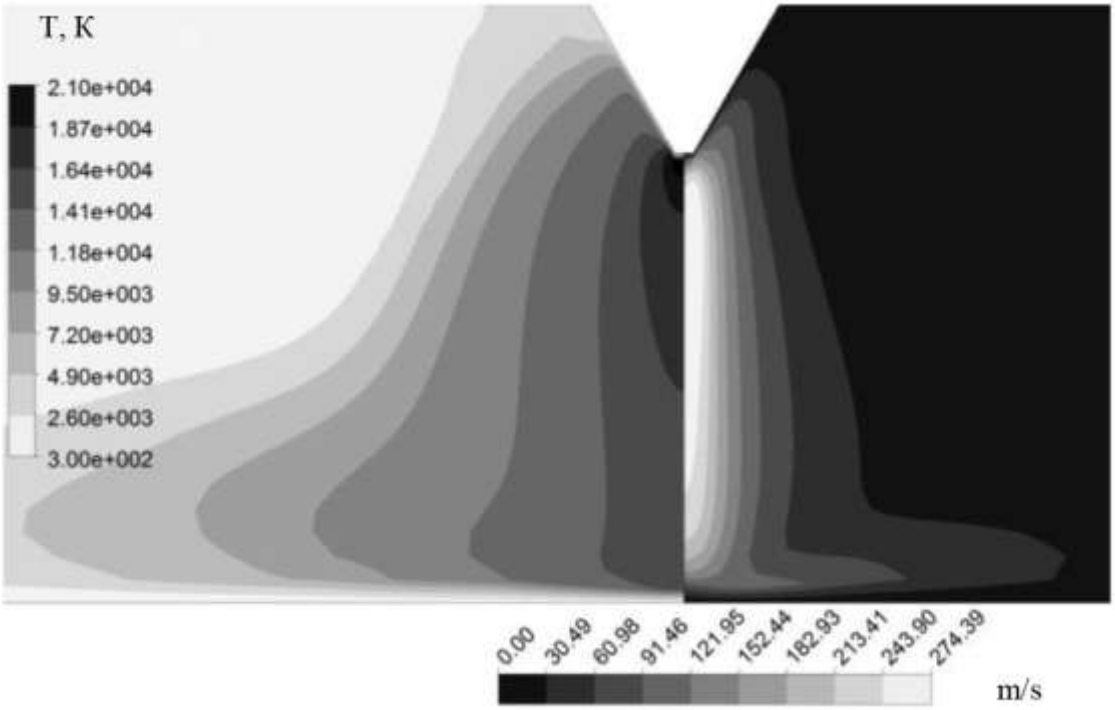


Figure 12 – Temperature field (left) and velocity field of argon plasma

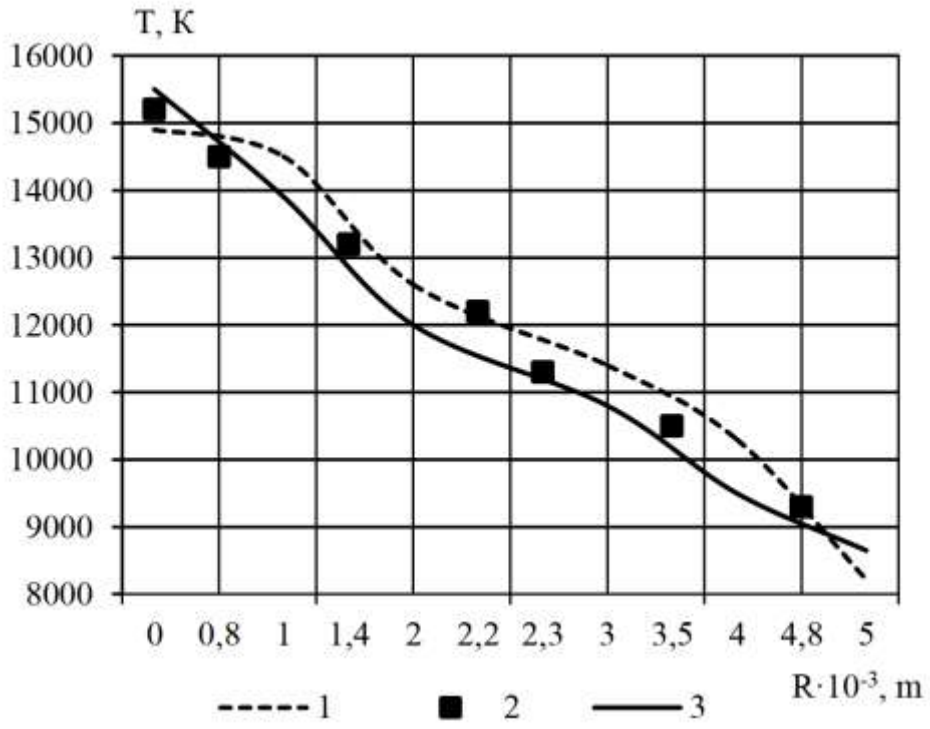


Figure 13 – Dependence of temperature on distance to cathode axis
1, 2 – existing experimental and calculated data;
3 – the author's results

Conclusions

1. The main approaches to mathematical simulation of physical processes in plasma have been analysed. It has been proposed and developed a mathematical model based on the magnetogasdynamic approach for describing plasma.
2. As a result of comparative analysis of existing turbulence models, as well as comparing simulation results with other authors and experiments, SAS - SST turbulence model has been selected, which most fully meets all the requirements for simulation of flows in the plasmatron channels.
3. It is shown that the results obtained within the gas-dynamic and magnetogasdynamic approaches differ significantly. Thus, the analysis of the atmosphere composition for the test problem showed a difference of three orders of magnitude for the values of partial pressure of oxygen-containing gases in the cathode sheath. The main mechanism of oxygen-containing gases penetration is the non-stationary behaviour of the electric arc. Moving of the arc roots contributes to formation of vortex structures and reverse flows towards cathode.
4. The comparative analysis of the results of simulation of a free-flaming electric arc of atmospheric pressure has shown an acceptable quantitative and qualitative agreement of the obtained result with the experimental data. The tolerance comprised up to 6% for temperature values and up to 3% for maximum velocity values at arc axis.

Bibliography

1. Нгуен Куок Ши. Исследование индукционных и дуговых плазмотронов [Текст]: дисс. … д-ра техн. наук: / Нгуен Куок Ши. – Санкт-Петербург, 2002. - 439 с.
2. Планковский, С.И. Научные основы создания высокоресурсных термоэмиссионных катодных узлов оборудования для плазменной обработки материалов [Текст]: дисс… д-ра техн. наук: 05.03.07 / Планковский Сергей Игоревич. – Харьков, 2009. – 333 с.
3. Соломатов, В.В. Математическое моделирование процессов в электродуговых генераторах низкотемпературной плазмы [Текст]: дис…канд. физ.-мат. наук: 05.13.18 / Соломатов Василий Владимирович; Институт вычислительных технологий РАН СО. – Новосибирск, 2003. – 148 с.
4. Ландау, Л.Д. Гидродинамика [Текст]/ Л.Д. Ландау, Е.М. Лившиц – М., 1980. – 535 с.
5. Jones, W.P. The prediction of laminarization with a two-equation model of turbulence [Текст] / W.P. Jones, B.E. Launder // Int. J. Heat and Mass Transfer. – 1972. – V.15. – P.301 – 314.
6. Алямовский, А.А. SolidWorks. Компьютерное моделирование в инженерной практике [Текст] / под ред.. А.А. Алямоского. – СПб.: БХВ Петербург, 2018 – 800 с.
7. Волков, Э.П. Моделирование горения твердого топлива [Текст] / Э.П. Волков, Л.И. Зайчик, В.А. Першуков. – М.: Наука, 1994. – 320 с.
8. Слободянюк, В.С. Моделирование вихревых и турбулентных явлений в электродуговых устройствах [Текст]: дис…д-ра техн. наук: 01.04.14 / Слободянюк Валерий Сергеевич. – Бишкек, 1996. – 376 с.
9. Menter, F.R. Two-equation eddy-viscosity turbulence models for engineering applications [Текст] / F.R. Menter // AIAA-Journal – 1994. – № 32(8). – P. 269 – 289.
10. Menter, F.R. A scale-adaptive simulation model for turbulent flow predictions [Текст] / F.R. Menter, M. Kuntz, R. Bender. – AIAA Paper 2003-0767, 2003. – 40 p.
11. Bradshaw, P. “Effects of Streamwise Curvature on turbulent Flow” [Текст] / P. Bradshaw. AGARD-AG-169, 1973.
12. Spalart, P.R. “On the sensitization of simple turbulence models to rotation and curva-ture” [Текст]/ P.R. Spalart, M.L. Shur // Aerospace Science and Technology, 1997, v. 1, No.5, pp 297-302.
13. Piomelli, U. “Wall-layer models for large-eddy simulations” [Текст] / U. Piomelli, E.

Balaras // Annual Rev. Fluid Mech., 2002, v.34, pp. 349-374.
14. Comments on the feasibility of LES for wings, and on a hybrid RANS/LES approach [Текст] / P.R. Spalart, W.H. Jou, M. Strelets, S.R. Allmaras // Proceedings of first AFOSR international conference on DND/LES, 1997.
15. Physical and numerical upgrades in the detached-eddy simulation of complex turbulent flows [Текс] / A. Travin, M. Shur, M. Strelets, P.R. Spalart // Proceedings of Euromech Coll. "LES of complex transitional and turbulent flows", Munich, Germany, 2002. Fluid Mechanics and Its Applications, 2004, v. 65, No. 5, pp. 239-254.
16. Davidson, L. "Evaluation of the SST-SAS model: channel flow, asymmetric diffuser and axi-symmetric hill" [Текст] / L. Davidson // European Conference on Computational Fluid Dynamics ECCOMAS CFD 2006.
17. Davidson, L. "A turbulence model with controlled modeled dissipation" 20th Nordic Seminar on Computational Mechanics [Текст] / L. Davidson. 20-23 Nov., 2007.
18. Юревич, Ф.Б. Электродуговой нагрев газа [Текст] / Ф.Б. Юревич, В.С. Куликов. – Минск: Наука и техника, 1973. – 192 с.
19. Варгафтик, Н.Б. Справочник по теплофизическим свойствам газов и жидкостей [Текст] / Н.Б. Варгафтик. – М.: Наука, 1972. – 721 с.
20. Hayashi, M. Recommended values of transport cross sections for elastic collisions and total collision cross section for electrons in atomic and molecular gases [Текст] / M. Hayashi. Report IPPJ AM. 1981.
21. Соколова, И.А. Процессы резонансного обмена в транспортных свойствах низкотемпературной плазмы. [Текст] / И.А. Соколова // Математическое моделирование. – 1989 - том 1. - № 3. - С. 84-99.
22. Anakhov S.V. Gas vortex stabilization in plasma torches: new solutions / S.V. Anakhov, Yu.A. Pykin, A.V. Matushkin // Welding International. - 2016. - Volume 30. - Issue 5. - p. 408-412
23. Devoto, R.S. Transport Coefficients of Ionized Argon [Текст] / R.S. Devoto // The Physics of Fluids. – 1973. – Vol. 16. – No. 5. – P. 616 – 623.
24. Костюк, Г.И. Исследование теплового и напряженного состояния в катодном пятне на электроде плазмотрона [Текст] / Г.И. Костюк, С.И. Планковский, С.Н. Лашко // Вопросы проектирования и производства конструкций летательных аппаратов: сб. науч. тр. Нац. аэрокосм. ун-та им. Н.Е. Жуковского «ХАИ». – Вып.3(54). – Х., 2008. – С. 148 – 162.
25. Гарин, В.О. Газодинамическое проектирование катодных узлов плазмотронов для утилизации полимерных композиционных материалов [Текст]: дис…канд. техн. наук: 05.03.07 / Гарин Вадим Олегович. – Харьков, 2012. – 148с.
26. Цегельник, Е.В. Обоснование параметров газодинамической защиты катодов плазмотронов для наземных испытаний летательных аппаратов [Текст]: дис…канд. техн. наук: 05.07.02 / Цегельник Евгений Владимирович. – Харьков, 2010. – 174с.
27. Брега, Д.А. Анализ существующих подходов к расчету газодинамической защиты катодных узлов плазмотронов [Текст] / Д.А. Брега, В.О. Гарин, С.И. Планковский // Вопросы проектирования и производства конструкций летательных аппаратов: сб. науч. тр. Нац. аэрокосм. ун-та им. Н.Е. Жуковского «ХАИ».– Вып. 73. – Х., 2013. – С. 122 – 128.
28. Lowke, J. LTE-diffusion approximation for arc calculations [Текст] / J. Lowke, M. Tanaka // J. Phys. D: Appl. Phys. – № 39, 2006. – P. 3634-3643.

Bibliography (transliterated)

1. Nguyen Kuok Shi. Issledovaniye induktsionnykh i dugovykh plazmotronov [Tekst]: disc. …

d-ra tekhn. nauk: / Nguyen Kuok Shi. – Sankt-Peterburg, 2002. - 439 s.
2. Plankovskiy, S.I. Nauchnyye osnovy sozdaniya vysokoresursnykh termoemissionnykh katodnykh uzlov oborudovaniya dlya plazmennoy obrabotki materialov [Tekst]: diss… d-ra tekhn. nauk: 05.03.07 / Plankovskiy Sergey Igorevich. – Kharkov, 2009. – 333 s.
3. Solomatov, V.V. Matematicheskoye modelirovaniye protsessov v elektrodugovykh generatorakh nizkotemperaturnoy plazmy [Tekst]: dis…kand. fiz.-mat. nauk: 05.13.18 / Solomatov Vasiliy Vladimirovich; Institut vychislitelnykh tekhnologiy RAN SO. – Novosibirsk, 2003. – 148 s.
4. Landau, L.D. Gidrodinamika [Tekst]/ L.D. Landau, Ye.M. Livshits – M., 1980. – 535 s.
5. Jones, W.P. The prediction of laminarization with a two-equation model of turbulence [Текст] / W.P. Jones, B.E. Launder // Int. J. Heat and Mass Transfer. – 1972. – V.15. – P.301 – 314.
6. Alyamovskiy, A.A. SolidWorks. Komp'yuternoye modelirovaniye v inzhenernoy praktike [Tekst] / pod red.. A.A. Alyamoskogo. – SPb.: BKHV Peterburg, 2018 – 800 s.
7. 7. Volkov, E.P. Modelirovaniye goreniya tverdogo topliva [Tekst] / E.P. Volkov, L.I. Zaychik, V.A. Pershukov. – M.: Nauka, 1994. – 320 s.
8. Slobodyanyuk, V.S. Modelirovaniye vikhrevykh i turbulentnykh yavleniy v elektrodugovykh ustroystvakh [Tekst]: dis…d-ra tekhn. nauk: 01.04.14 / Slobodyanyuk Valeriy Sergeyevich. – Bishkek, 1996. – 376 s.
9. Menter, F.R. Two-equation eddy-viscosity turbulence models for engineering applications [Текст] / F.R. Menter // AIAA-Journal – 1994. – № 32(8). – P. 269 – 289.
10. Menter, F.R. A scale-adaptive simulation model for turbulent flow predictions [Текст] / F.R. Menter, M. Kuntz, R. Bender. – AIAA Paper 2003-0767, 2003. – 40 p.
11. Bradshaw, P. “Effects of Streamwise Curvature on turbulent Flow” [Текст] / P. Bradshaw. AGARD-AG-169, 1973.
12. Spalart, P.R. “On the sensitization of simple turbulence models to rotation and curva-ture” [Текст]/ P.R. Spalart, M.L. Shur // Aerospace Science and Technology, 1997, v. 1, No.5, pp 297-302.
13. Piomelli, U. “Wall-layer models for large-eddy simulations” [Текст] / U. Piomelli, E. Balaras // Annual Rev. Fluid Mech., 2002, v.34, pp. 349-374.
14. Comments on the feasibility of LES for wings, and on a hybrid RANS/LES approach [Текст] / P.R. Spalart, W.H. Jou, M. Strelets, S.R. Allmaras // Proceedings of first AFOSR international conference on DND/LES, 1997.
15. Physical and numerical upgrades in the detached-eddy simulation of complex turbulent flows [Текс] / A. Travin, M. Shur, M. Strelets, P.R. Spalart // Proceedings of Euromech Coll. “LES of complex transitional and turbulent flows”, Munich, Germany, 2002. Fluid Mechanics and Its Applications, 2004, v. 65, No. 5, pp. 239-254.
16. Davidson, L. “Evaluation of the SST-SAS model: channel flow, asymmetric diffuser and axi-symmetric hill” [Текст] / L. Davidson // European Conference on Computational Fluid Dynamics ECCOMAS CFD 2006.
17. Davidson, L. “A turbulence model with controlled modeled dissipation” 20th Nordic Seminar on Computational Mechanics [Текст] / L. Davidson. 20-23 Nov., 2007.
18. Yurevich, F.B. Elektrodugovoy nagrev gaza [Tekst] / F.B. Yurevich, V.S. Kulikov. – Minsk: Nauka i tekhnika, 1973. – 192 s.
19. Vagraftik, N.B. Spravochnik po teplofizicheskim svoystvam gazov i zhidkostey [Tekst] / N.B. Vargaftik. – M.: Nauka, 1972. – 721 s.
20. Hayashi, M. Recommended values of transport cross sections for elastic collisions and total collision cross section for electrons in atomic and molecular gases [Tekst] / M. Hayashi. Report IPPJ AM. 1981.
21. Sokolova, I.A. Protsessy rezonansnogo obmena v transportnykh svoystvakh nizkotemperaturnoy plazmy. [Tekst] / I.A. Sokolova // Matematicheskoye modelirovaniye. –

1989 - tom 1. - № 3. - S. 84-99.
22. Anakhov S.V. Gas vortex stabilization in plasma torches: new solutions / S.V. Anakhov, Yu.A. Pykin, A.V. Matushkin // Welding International. - 2016. - Volume 30. - Issue 5. - p. 408-412
23. Devoto, R.S. Transport Coefficients of Ionized Argon [Текст] / R.S. Devoto // The Physics of Fluids. – 1973. – Vol. 16. – No. 5. – P. 616 – 623.
24. Kostyuk, G.I. Issledovaniye teplovogo i napryazhennogo sostoyaniya v katodnom pyatne na elektrode plazmotrona [Tekst] / G.I. Kostyuk, S.I. Plankovskiy, S.N. Lashko // Voprosy proyektirovaniya i proizvodstva konstruktsiy letatelnykh apparatov: sb. nauch. tr. Nats. aerokosm. un-ta im. N.Ye. Zhukovskogo «KHAI». – Vyp.3(54). – KH., 2008. – S. 148 – 162.
25. Garin, V.O. Gazodinamicheskoye proyektirovaniye katodnykh uzlov plazmotronov dlya utilizatsii polimernykh kompozitsionnykh materialov [Tekst]: dis…kand. tekhn. nauk: 05.03.07 / Garin Vadim Olegovich. – Khar'kov, 2012. – 148s.
26. Tsegelnik, Ye.V. Obosnovaniye parametrov gazodinamicheskoy zashchity katodov plazmotronov dlya nazemnykh ispytaniy letatelnykh apparatov [Tekst]: dis…kand. tekhn. nauk: 05.07.02 / Tsegelnik Yevgeniy Vladimirovich. – Kharkov, 2010. – 174s.
27. Brega, D.A. Analiz sushchestvuyushchikh podkhodov k raschetu gazodinamicheskoy zashchity katodnykh uzlov plazmotronov [Tekst] / D.A. Brega, V.O. Garin, S.I. Plankovskiy // Voprosy proyektirovaniya i proizvodstva konstruktsiy letatelnykh apparatov: sb. nauch. tr. Nats. aerokosm. un-ta im. N.Ye. Zhukovskogo «KHAI».– Vyp. 73. – KH., 2013. – S. 122 – 128.